ADA082371

LEVEL II

2

6 REENTRY ANTENNA TEST (RANT) PROGRAM. [redacted]

[redacted]

Volume II.

LINEAR PLASMA MODEL.

[redacted] (ADDENDUM).

NH

Prepared by

AVCO GOVERNMENT PRODUCTS GROUP
AVCO SYSTEMS DIVISION
201 Lowell Street
Wilmington, Massachusetts, 01887

9 Preliminary rept.,

10 R. L. Fante R. Elkin J. Gottesfeld R. O'Keefe

AVSD-0374-69-CR, Add[redacted]

15 Contract F04701-68-C-0283

11 25 Mar[redacted]70

14 AVSD-0374-69-CR-VOL-2-ADD

12 63

NH

Prepared for

SPACE AND MISSILE SYSTEMS ORGANIZATION
AIR FORCE SYSTEMS COMMAND
Norton Air Force Base, California 92409

ADDENDUM TO RANT PRELIMINARY REPORT

VOLUME II

7420956L

Prepared by

AVCO GOVERNMENT PRODUCTS GROUP
AVCO SYSTEMS DIVISION
201 Lowell Street
Wilmington, Massachusetts 01887

Dr. R. L. Fante
Principal Investigator

Contributors

Dr. R. Elkin, Programming
J. Gottesfeld, Programming
R. O'Keefe, Programming

Contract F04701-68-C-0283

25 March 1970

Approved

E. D. Shane
Associate Program Manager

R. W. Wilson
Program Manager

Prepared for

SPACE AND MISSILE SYSTEMS ORGANIZATION
AIR FORCE SYSTEMS COMMAND
Norton Air Force Base, California 92409

FOREWORD

This report was prepared by Avco Corporation/Systems Division under the terms of the Reentry Antenna Test (RANT) Program, Air Force Contract No. F04701-68-C-0283. It is submitted as part of the Preliminary Design Review (PDR) package, in partial fulfillment of the contract and in accordance with Contract Data Requirements List (CDRL) Item No. 6. The report is an addendum to a corresponding report submitted at the Systems Studies Review.

The program is administered under the direction of the Space and Missile Systems Organization (SAMSO) with Captain J. Van Zale as Project Officer. Mr. C. Okerstrom, Manager, Aerospace Corporation Flight Test Vehicles Project Office and Mr. R. A. Mills, Manager, Aerospace Corporation Electronic Countermeasures Project Office were the principle technical monitors for the work reported.

TABLE OF CONTENTS

LIST OF ILLUSTRATIONS

LIST OF TABLES

1.0 Introduction

In Volume 2 of the RANT preliminary report we discussed the ground plane model for predicting the effect of a reentry plasma on aperture antennas. In that volume we also began the discussion of the cylinder model, (i.e., apertures on a plasma covered infinite cylinder). In this volume we conclude the discussion of the cylinder model. However, for completeness, we repeat some of the discussion contained in Volume 2.

In modeling the plasma the effects of high temperatures have been intentionally omitted. Their inclusion would substantially increase the complexity of the calculations without significant compensatory gain in accuracy. Analysis indicated that the error contribution would be essentially small (only a few percentage points) at the electron densities, collision frequencies, and temperatures of interest.

In both models the plasma is approximated by a dielectric whose local dielectric constant is (all analysis and results assume $e^{-i\omega t}$, except for Tables I, II and III where an $e^{j\omega t}$ is assumed for purposes of comparison)

$$\epsilon = \left(1 - \frac{\omega_p^2}{\omega^2 + \nu_c^2}\right) + i\left(\frac{\nu_c}{\omega}\right)\left(\frac{\omega_p^2}{\omega^2 + \nu_c^2}\right)$$

where

ϵ = local dielectric constant

ω_p = electron plasma frequency

ν_c = electron-neutral collision frequency

ω = radian signal frequency

The collision frequency ν_c is assumed to be independent of field strength. A discussion of this approximation is given in Section 3.0.

2.0 Cylinder Linear Plasma Model

2.1 Analysis

The second linear plasma model considers apertures (either axial or circumferential) on an infinite perfectly conducting cylinder. Again we assume that the apertures are excited in the dominant mode and that the inhomogeneous plasma is approximated by a series of thin layers, each of which is individually homogeneous, as shown in Figure 1a.

By assuming appropriate expressions for the fields in each layer and applying the boundary conditions on the tangential fields across the boundaries of each layer and across the aperture/heat shield interface, we can obtain the following expressions for the self and mutual admittances

$$Y_{11} = (2\pi)^{2} \sum_{n=-\infty}^{\infty} \int_{-\infty}^{\infty} d\alpha \, \hat{\underline{e}}_0^{*}(n,\alpha) \cdot \underset{\sim}{C}_n(\alpha) \cdot \hat{\underline{e}}_0(n,\alpha) \tag{1}$$

$$Y_{12} = (2\pi)^{2} \sum_{n=-\infty}^{\infty} \int_{-\infty}^{\infty} d\alpha \, \hat{\underline{e}}_0^{*}(n,\alpha) \cdot \underset{\sim}{C}_n(\alpha) \cdot \hat{\underline{e}}_0(n,\alpha)\, e^{-i(n\phi_1 + \alpha z_1)} \tag{2}$$

where

$$\underset{\sim}{c}_n(\alpha) = \underline{i}_z \underline{i}_z I_n - \underline{i}_z \underline{i}_\phi J_n + \underline{i}_\phi \underline{i}_z G_n + \underline{i}_\phi \underline{i}_\phi K_n$$

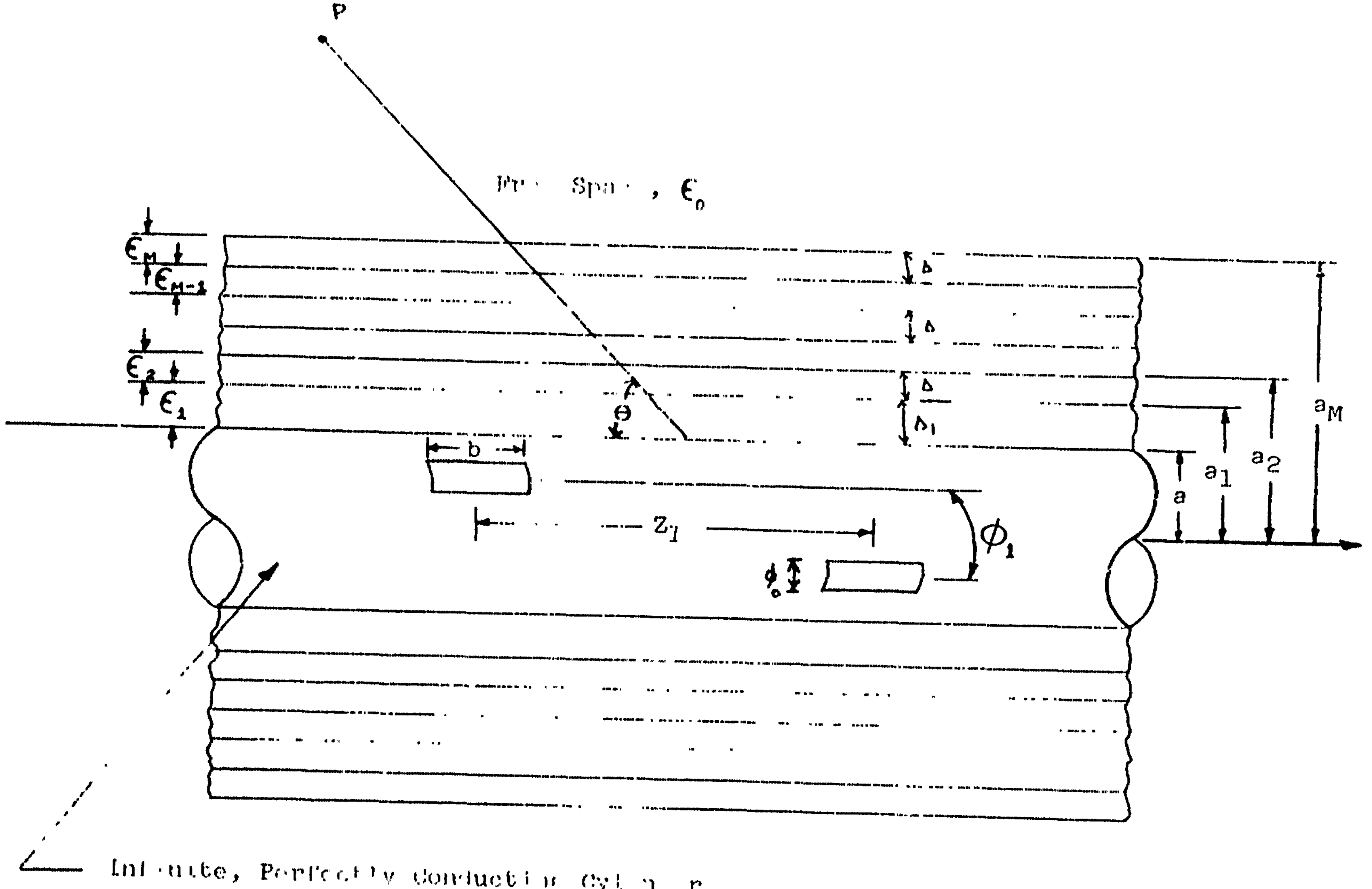

Figure 1a [illegible] (AXIAL SLOTS)

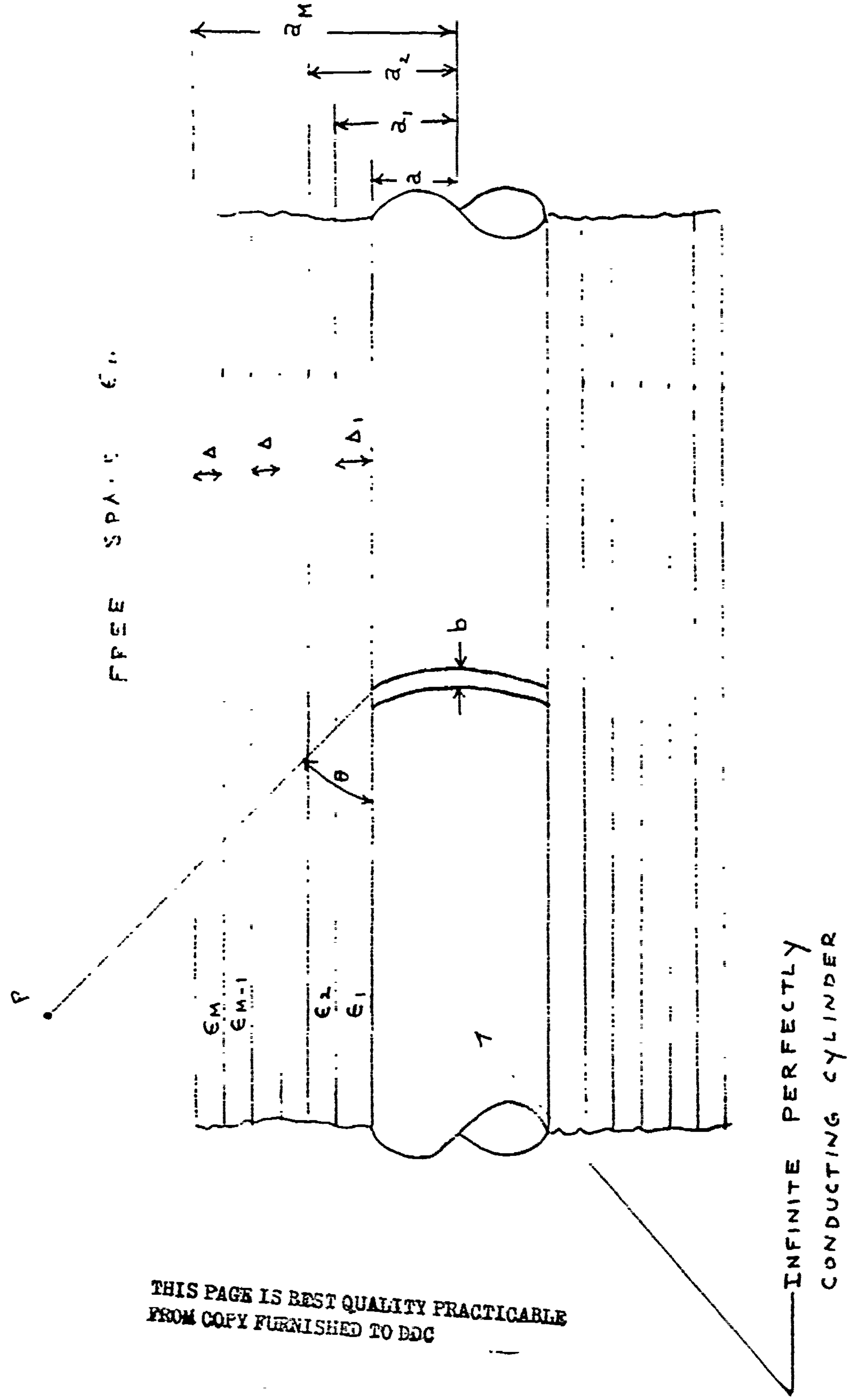

FIG 1b : CYLINDER MODEL (CIRCUMFERENTIAL GAP)

$$\hat{\mathcal{E}}_0(n,\alpha) = \frac{1}{(2\pi)^2}\int_{-\pi}^{\pi} d\phi \int_{-\infty}^{\infty} dz\, e^{-i(n\phi+\alpha z)}\, \mathcal{E}_0(z,\phi)$$

$\mathcal{E}_0(z,\phi)$ = aperture field distribution (dominant mode)

$$I_n = \frac{\hat{q}_n t_n - \hat{t}_n q_n}{\Omega_n} \tag{3}$$

$$P_n = \frac{\hat{t}_n r_n - s_n \hat{q}_n}{\Omega_n} \tag{4}$$

$$Q_n = \frac{\hat{r}_n t_n - \hat{s}_n q_n}{\Omega_n} \tag{5}$$

$$T_n = \frac{(-\hat{r}_n r_n + \hat{s}_n s_n)}{\Omega_n} \tag{6}$$

$$r_n = l_1^2 \left[J_n(l_1 a) + \Gamma_n(\alpha) H_n(l_1 a)\right]$$

$$s_n = l_1^2 \Lambda_n(\alpha) H_n(l_1 a)$$

$$q_n = (n\alpha/a)\left[J_n(l_1 a) + \Gamma_n(\alpha) H_n(l_1 a)\right] + i\omega\mu_0 l_1 H_n'(l_1 a) U_n(\alpha)$$

$$t_n = (n\alpha/a)\Lambda_n(\alpha) H_n(l_1 a) + i\omega\mu_0 l_1 \left[J_n'(l_1 a) + V_n(\alpha) H_n'(l_1 a)\right]$$

$$\hat{r}_n = l_1^2 H_n(l_1 a) U_n(\alpha)$$

$$\hat{s}_n = l_1^2 \left[J_n(l_1 a) + V_n(\alpha) H_n(l_1 a)\right]$$

$$\hat{q}_n = i\omega\epsilon_1 l_1 \left[J_n'(l_1 a) + \Gamma_n(\alpha) H_n'(l_1 a)\right] - (n\alpha/a) H_n(l_1 a) U_n$$

$$\hat{t}_n = i\omega\epsilon_1 l_1 H_n'(l_1 a)\Lambda_n(\alpha) - (n\alpha/a)\left[J_n(l_1 a) + V_n(\alpha) H_n(l_1 a)\right]$$

$$\Omega_n = t_n \xi_n - q_n \varepsilon_n$$

$$\Gamma_n = \left(\frac{T_{24} T_{32} - T_{22} T_{34}}{\Delta}\right)$$

$$\Lambda_n = \left(\frac{T_{22} T_{14} - T_{12} T_{24}}{\Delta}\right)$$

$$U_n = \left(\frac{T_{44} T_{32} - T_{42} T_{34}}{\Delta}\right)$$

$$V_n = \left(\frac{T_{14} T_{42} - T_{44} T_{12}}{\Delta}\right)$$

$$\Delta = T_{32} T_{14} - T_{12} T_{34}$$

$$l_m = \sqrt{\epsilon_m k_o^2 - \alpha^2}$$

J_n, Y_n = Bessel and Neumann functions

$[T]$ = the 4 x 4 matrix:

$$[T] = \begin{bmatrix} T_{11} & T_{12} & T_{13} & T_{14} \\ T_{21} & T_{22} & T_{23} & T_{24} \\ T_{31} & T_{32} & T_{33} & T_{34} \\ T_{41} & T_{42} & T_{43} & T_{44} \end{bmatrix}$$

this, in turn, is defined as

$$[T] = \prod_{m=1}^{M_1} \left[Q_n(m) \right]$$

For $m \neq M$, but valid for $m = 1, 2, \ldots M-1$, we have:

$$Q_n(m) = \frac{1}{i l_m^2} \begin{bmatrix} \alpha_{nm} & \beta_{nm} & \gamma_{nm} & \delta_{nm} \\ \rho_{nm} & \hat{s}_{nm} & \vartheta_{nm} & \phi_{nm} \\ \bar{a}_{nm} & b_{nm} & c_{nm} & d_{nm} \\ e_{nm} & f_{nm} & g_{nm} & h_{nm} \end{bmatrix}$$

with

$$\rho_{nm} = \frac{\pi a_m \ell_m \ell_{m+1}}{2\,\epsilon_m}\Big[\epsilon_{m+1}\ell_m J_n(X_m)\, J_n'(\bar{X}_{m+1}) - \epsilon_m \ell_{m+1} J_n'(X_m)\, J_n(\bar{X}_{m+1})\Big]$$

$$\xi_{nm} = \frac{\pi a_m \ell_m \ell_{m+1}}{2\,\epsilon_m}\Big[\epsilon_{m+1}\ell_m J_n(X_m)\, H_n'(\bar{X}_{m+1}) - \epsilon_m \ell_{m+1} J_n'(X_m)\, H_n(\bar{X}_{m+1})\Big]$$

$$\bar{a}_{nm} = \frac{i n \pi \alpha}{2\,\omega\mu_0} H_n(X_m)\, J_n(\bar{X}_{m+1})\Big[\ell_m^2 - \ell_{m+1}^2\Big]$$

$$b_{nm} = \frac{i n \pi \alpha}{2\,\omega\mu_0} H_n(X_m)\, H_n(\bar{X}_{m+1})\Big[\ell_m^2 - \ell_{m+1}^2\Big]$$

$$c_{nm} = -(\pi/2)\,\ell_m \ell_{m+1} a_m\Big[\ell_m J_n'(\bar{X}_{m+1})\, H_n(X_m) - \ell_{m+1} J_n(\bar{X}_{m+1})\, H_n'(X_m)\Big]$$

$$d_{nm} = -(\pi/2)\,\ell_m \ell_{m+1} a_m\Big[\ell_m H_n'(\bar{X}_{m+1})\, H_n(X_m) - \ell_{m+1} H_n(\bar{X}_{m+1})\, H_n'(X_m)\Big]$$

$$e_{nm} = \frac{-i n \pi \alpha}{2\,\omega\mu_0}\left(\ell_m^2 - \ell_{m+1}^2\right) J_n(X_m)\, J_n(\bar{X}_{m+1})$$

$$f_{nm} = \frac{-i n \pi \alpha}{2\,\omega\mu_0}\left(\ell_m^2 - \ell_{m+1}^2\right) J_n(X_m)\, H_n(\bar{X}_{m+1})$$

$$g_{nm} = (\pi/2)\,\ell_m \ell_{m+1} a_m\Big[\ell_m J_n(X_m)\, J_n'(\bar{X}_{m+1}) - \ell_{m+1} J_n'(X_m)\, J_n(\bar{X}_{m+1})\Big]$$

$$h_{nm} = (\pi/2)\, l_m\, l_{m+1}\, a_m \left[l_m J_n(X_m)\, H_n'(\bar{X}_{m+1}) - l_{m+1} J_n'(X_m)\, H_n(\bar{X}_{m+1}) \right]$$

$$\alpha_{nm} = -(\pi/2) \frac{l_m l_{m+1} a_m}{\epsilon_m} \left[\epsilon_{m+1} l_m H_n(X_m)\, J_n'(\bar{X}_{m+1}) - \epsilon_m l_{m+1} H_n'(X_m)\, J_n(\bar{X}_{m+1}) \right]$$

$$\beta_{nm} = -(\pi/2) \frac{l_m l_{m+1} a_m}{\epsilon_m} \left[\epsilon_{m+1} l_m H_n(X_m)\, H_n'(\bar{X}_{m+1}) - \epsilon_m l_{m+1} H_n'(X_m)\, H_n(\bar{X}_{m+1}) \right]$$

$$\gamma_{nm} = - \left(\frac{\mu_0}{\epsilon_m \epsilon_0} \right) \bar{a}_{nm}$$

$$\delta_{nm} = - \left(\frac{\mu_0}{\epsilon_m \epsilon_0} \right) b_{nm}$$

$$\theta_{nm} = - \left(\frac{\mu_0}{\epsilon_m \epsilon_0} \right) e_{nm}$$

$$\phi_{nm} = - \left(\frac{\mu_0}{\epsilon_m \epsilon_0} \right) f_{nm}$$

$$X_m = l_m a_m$$

$$\bar{X}_{m+1} = l_{m+1} a_m$$

When m = M, which corresponds to the free space beyond the plasma,

$$Q_n(M) = \frac{1}{i\, l_M^2} \begin{bmatrix} 0 & \beta_{nM} & 0 & \delta_{nM} \\ 0 & \xi_{nM} & 0 & \phi_{nM} \\ 0 & b_{nM} & 0 & d_{nM} \\ 0 & f_{nM} & 0 & h_{nM} \end{bmatrix}$$

with

$$b_{nM} = \frac{i n \pi \alpha}{2 \omega \mu_0} H_n(X_M) H_n(\ell_0 a_M) \left[\ell_M^2 - \ell_0^2\right]$$

$$d_{nM} = -(\pi/2)\ell_0 \ell_M a_M \left[\ell_M H_n(X_M) H_n'(\ell_0 a_M) - \ell_0 H_n(\ell_0 a_M) H_n'(X_M)\right]$$

$$\xi_{nM} = \frac{\pi a_M \ell_0 \ell_M}{2 \epsilon_M} \left[\ell_M J_n(X_M) H_n'(\ell_0 a_M) - \epsilon_M \ell_0 J_n'(X_M) H_n(\ell_0 a_M)\right]$$

$$\phi_{nM} = \frac{i n \pi \alpha}{2 \omega \epsilon_0 \epsilon_M} (\ell_M^2 - \ell_0^2) J_n(X_M) H_n(\ell_0 a_M)$$

$$\eta_{nM} = \frac{-\ell_0 \ell_M \pi a_M}{2 \epsilon_M} \left[\ell_M H_n(X_M) H_n'(\ell_0 a_M) - \epsilon_M \ell_0 H_n'(X_M) H_n(\ell_0 a_M)\right]$$

$$\delta_{nM} = \frac{-i n \pi \alpha}{2 \omega \epsilon_0 \epsilon_M} (\ell_M^2 - \ell_0^2) H_n(X_M) H_n(\ell_0 a_M)$$

$$f_{nM} = \frac{-i n \pi \alpha}{2 \omega \mu_0} (\ell_M^2 - \ell_0^2) J_n(X_M) H_n(\ell_0 a_M)$$

$$h_{nM} = (\pi/2) \ell_0 \ell_M a_M \left[\ell_M J_n(X_M) H_n'(\ell_0 a_M) - \ell_0 H_n(\ell_0 a_M) J_n'(X_M)\right]$$

$$X_m = \ell_m a_m , \quad \ell_0 = \sqrt{k_0^2 - \alpha^2}$$

and $H_n(z) = J_n(z) + i\,Y_n(z)$. A discussion of the technique used to compute the Bessel and Neumann functions for arbitrary complex arguments is given in Section 2.3. It is assumed in equations (1) and (2) that the apertures are identical, and that the aperture field distribution is the dominant mode.

For the case of two axial rectangular slots, as shown in Figure 1a, with each aperture distribution given by

$$\underline{e}_\phi = \sqrt{\frac{2}{ab\phi_0}} \cos\left(\frac{\pi z}{b}\right) \underline{i}_\phi$$

equations (1) and (2) reduce to

$$Y_{11} = (2\pi^2)\, a \sum_{n=-\infty}^{\infty} \int_{-\infty}^{\infty} d\alpha \, \left| \hat{e}_\phi(n,\alpha) \right|^2 K_n(\alpha) \tag{7}$$

$$Y_{12} = (2\pi)^2 a \sum_{n=-\infty}^{\infty} \int_{-\infty}^{\infty} d\alpha \, \left| \hat{e}_\phi(n,\alpha) \right|^2 K_n(\alpha)\, e^{-i(n\phi_1 + \alpha z_1)} \tag{8}$$

with K_n given by eqn (6), and

$$\hat{e}_\phi(n,\alpha) = \frac{\frac{1}{n\pi b}\sqrt{\frac{2}{ab\phi_0}} \sin\left(\frac{n\phi_0}{2}\right)\cos\left(\frac{b\alpha}{2}\right)}{\left(\frac{\pi}{b}\right)^2 - \alpha^2}$$

For a single circumferential gap executed by a uniform z-directed electric field, as shown in Figure 1b, equation (1) becomes

$$Y_{11} = -\frac{b}{2\pi}\int_{-\infty}^{\infty} d\alpha \, \frac{\sin^2\left(\frac{b\alpha}{2}\right)}{\left(\frac{b\alpha}{2}\right)^2} I_0(\alpha) \tag{9}$$

where $I_o(\alpha)$ is given by equation (3), and the contour of integration is indented above any singularities on the negative $Re(\alpha)$ axis and below any singularities on the positive $Re(\alpha)$ axis. The assumption that the exciting field is independent of ϕ, means that (9) is not valid for cylinders with a large ka.

The single axial slot radiation problem is solved by applying the method of steepest descent. Thus, we obtain for the radial component of the Poynting vector

$$
\begin{aligned}
N_R &= E_\theta H_\phi^* - E_\phi H_\theta^* \\
&= \frac{4k^3 \omega \epsilon_0}{r^2} \sin^2\theta \left[\left| \sum_{n=-\infty}^{\infty} L_n e^{i(n\phi - \psi_n)} \right|^2 \right. \\
&\qquad \left. + \frac{\mu_0}{\epsilon_0} \left| \sum_{n=-\infty}^{\infty} N_n e^{i(n\phi - \psi_n)} \right|^2 \right]
\end{aligned}
\tag{10}
$$

where

$$L_n = - \left\{ \frac{1}{\Omega_n \Delta} \left[T_{14} r_n + T_{34} s_n \right] \hat{e}_\phi(n,\alpha) \right\}_{\alpha = k\cos\theta}$$

$$N_n = \left\{ \frac{1}{\Omega_n \Delta} \left[T_{32} s_n + T_{12} r_n \right] \hat{e}_\phi(n,\alpha) \right\}_{\alpha = k\cos\theta}$$

$$\psi_n = \left(\frac{2n+1}{4} \right) \pi$$

It is not possible, in the case of two excited axial slots on the cylinder, to define an array factor as was done in the ground plane model. However, the radiation pattern (neglecting mutual coupling) can be obtained by replacing the term $\hat{e}_\phi(n, \alpha)$ in the definitions of L_n and N_n, above, by the term

$$\hat{e}_2(n,\alpha) = \hat{e}_\phi(n,\alpha)\left[1 + e^{-i(\lambda_p + n\phi_1 + \alpha z_1)}\right]$$

where

λ_p = phase difference between the excitations of the two slots

For the circumferential gap the radiation pattern is given by

$$R_g = \sin^2\theta \left[\frac{\sin\left(\frac{kb\cos\theta}{2}\right)}{\frac{kb\cos\theta}{2}}\right]^2 \left|\frac{T_{14}\,g_0 + T_{34}\,t_0}{\Omega_0\,\Delta}\right|^2_{\alpha = k\cos\theta} \tag{11}$$

Equations (10) and (11) are not valid for $\theta = o$. This is because in deriving (10) and (11) we have used the asymptotic expansion for $H_n(kr\sin\theta)$ which is not valid for $\theta = o$. (In addition as $\theta \to o$ the saddle point approaches a singularity, so that the usual saddle point expression would not be valid in any case.)

2.2 Discussion of Cylinder Linear Plasma Computer Program

Using all the above results, Avco Computer Program 2817 was developed. It has four options as follows:

(a) Option 1 computes Y_{11}, Y_{12}, and isolation for a pair of identical axial slots on an infinite cylinder covered by an arbitrary inhomogeneous plasma. (The plasma may be lossy or lossless.)

(b) Option 2 computes the radiation pattern for both a single and axial slot and for a pair of axial slots.

(c) Option 3 uses eqn (9) to compute the admittance of a circumferential gap on an infinite cylinder covered by an arbitrary inhomogeneous plasma.

(d) Option 4 calculates the radiation pattern for the above situation.

A complete Fortran Listing for program 2817 is contained in a separate volume. A typical input sheet and explanation of inputs is contained in Appendix III.

2.2.1 Verification and Results from Options 1 and 2

To verify the results of program 2817, we have compared its results with some results obtained by NASA, and also, where applicable, with ground plane results.

Table I compares the values provided by a computer program with similar values provided by a computer programs developed by C. Knop (1965) for the NASA Langley Research Center. The antenna considered in this case was a axial rectangular slot ($a\,\phi_o = .1687$ and $b = 2.38$) located on an infinite cylinder of radius $a = 1$ covered by a homogeneous plasma of thickness Δ_1, and dielectric constant ϵ_1. One may note from Table I that the comparison is reasonably good. The study presently being performed by Golden and Stewart (1969) of Aerospace will afford additional test cases in the future.

To examine the case when ϵ is complex we take $a = 3.6$, $b = 8.5$, $k = .418$, $\epsilon_1 = 1 + i\,20$, and $\Delta_1 = .0534$. In this case we expect that the thin sheath approximation is valid (Fante, 1967), and that $Y_{11} = Y_{11}^{(o)} + Y_s$, where $Y_{11}^{(o)}$ is the free space admittance and $Y_s = i\,k\Delta_1\ (\epsilon - 1)(120\pi)^{-1}$. (The error in using the above formula for the present example is of order 12%). Using

TABLE I

COMPARISON OF ADMITTANCES FOR AN AXIAL SLOT ON A PLASMA COVERED CYLINDER

ϵ_1	Δ_1	k	CONDUCTANCE		SUSCEPTANCE	
			Avco[1]	NASA[2]	Avco[1]	NASA[2]
.4	.01	1.5	1.50×10^{-4}	1.48×10^{-4}	-1.54×10^{-4}	-1.52×10^{-4}
.7	.01	1.5	1.52×10^{-4}	1.52×10^{-4}	-1.92×10^{-4}	-1.88×10^{-4}

1 - From Avco computer program 2817

2 - NASA Langley Computer Program by C. Knop

the thin sheath approximation we find that

$$Y_{11} = 1.33 \times 10^{-3} - i\,.210 \times 10^{-3} \qquad \text{mho}$$

while program 2817 calculates

$$Y_{11} = 1.27 \times 10^{-3} - i\,.24 \times 10^{-3} \qquad \text{mho}$$

Since the value calculated by 2817 agrees with the thin sheath result (to within the error inherent in the thin sheath approximation) we conclude that program 2817 is also operating satisfactorily for the case of complex ϵ .

It is also desirable to study the isolation results predicted by program 2817. Figure 2 shows the isolation of two axial slots. The upper curve shows the change in H-plane isolation as a function of separation, while the lower curve describes the change in E-plane isolation as the azimuthal separation ϕ_1 is varied. As expected the isolation increases with increasing slot separation.

Figure 3 shows the cnange in E-plane isolation for a cylinder covered by a two layer plasma. For this case the computed self-admittance is $Y_{11} = .758 \times 10^{-2} + i\,.118 \times 10^{-2}$. It should be pointed out that in this example the sum over n (the azimuthal modes) was terminated at N = 101 due to computer underflows. Generally, for small isolations (i.e., isolations less than about 80 db) this does not present any problem. However, for cases when the isolation is large, and hence Y_{12} very small, it is possible that the neglected terms (i.e., $\sum_{N}^{\infty}\int_{-\infty}^{\infty} d\alpha\, K_n(\alpha) \ldots$) may be of the same order as the computed answer. Then, the computed isolations should be regarded in an

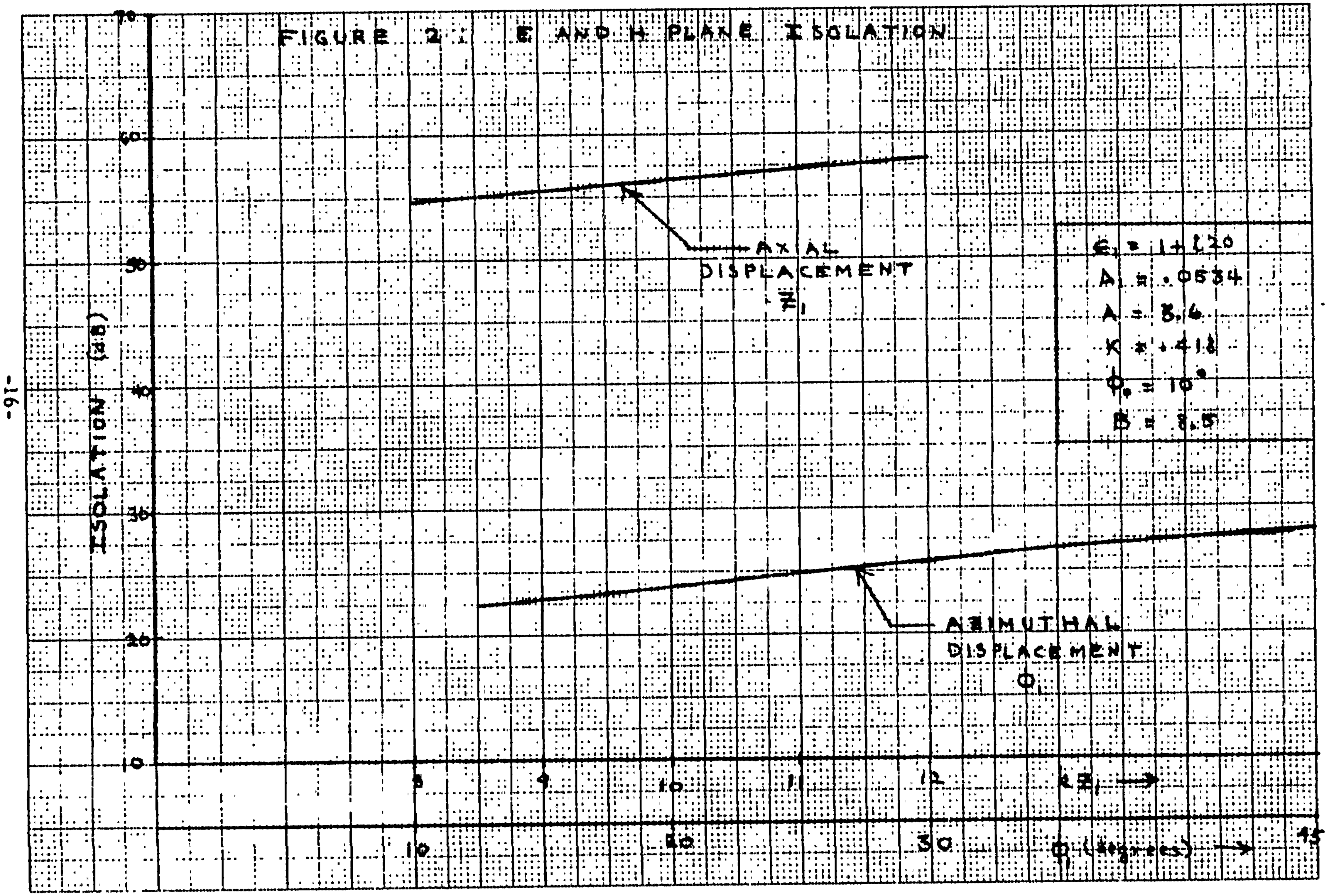

FIGURE 2.1 E AND H PLANE ISOLATION

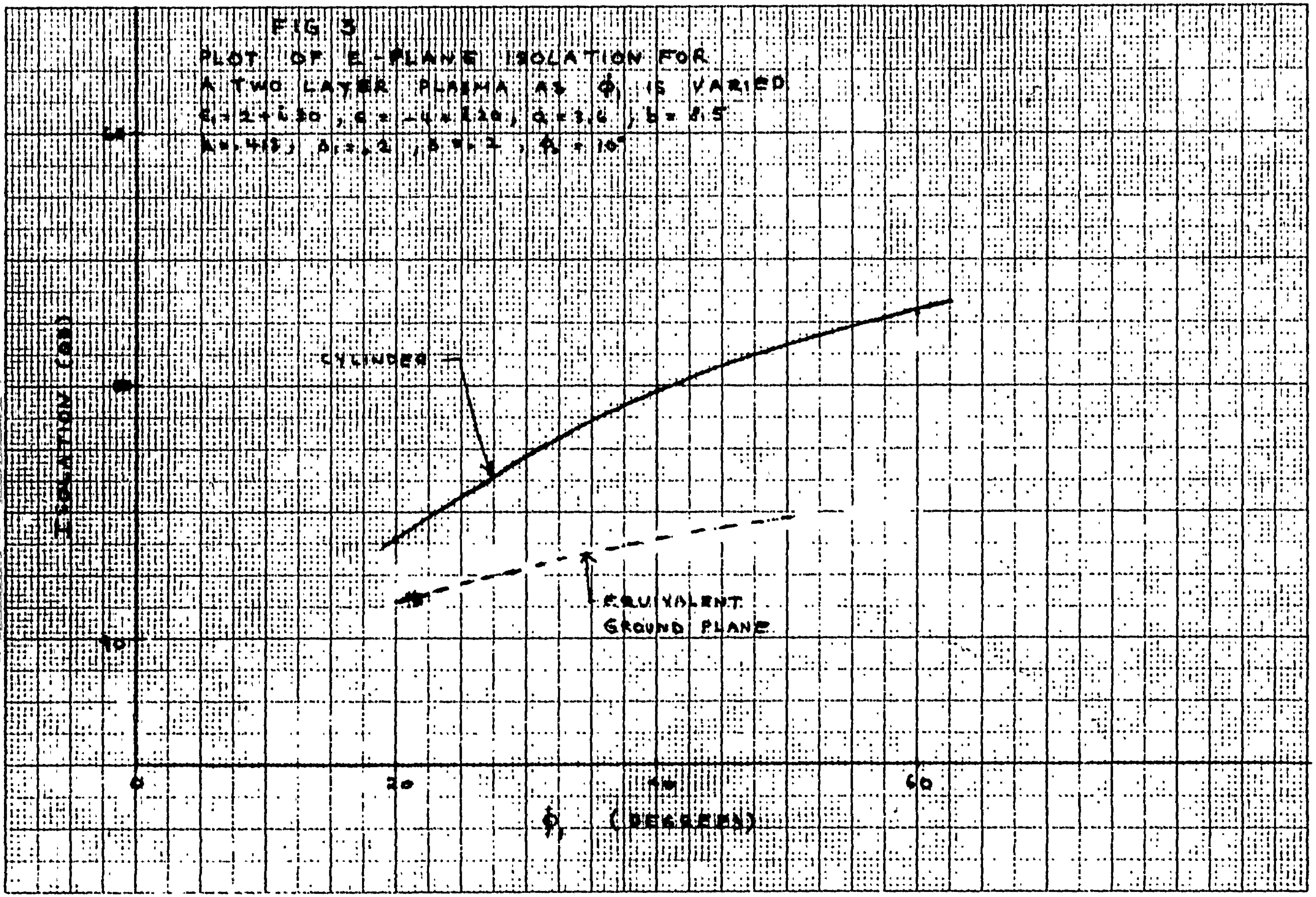
FIG 3
PLOT OF E-PLANE ISOLATION FOR
A TWO LAYER PLASMA AS Φ_1 IS VARIED
CYLINDER
EQUIVALENT
GROUND PLANE
ISOLATION (DB)
10
0
20
40
60
Φ_1 (DEGREES)

order of magnitude sense, and may possibly be a few db different from the answer one would obtain if the $\sum_{n}$ were not truncated ... 101. (The neglected terms are especially important for cases when ϕ_1 is large since there then arises cancellation for small n from term to term in the summation $\sum_n e^{in\phi_1} F(m)$ in eqn (8), so that the large n terms assume increasing importance.) Fortunately, in practical situations we do not need extremely accurate results when the isolation is large.

It is also interesting to conjecture how the H-plane admittance and isolation (for this case $\phi_1 = o$) between two axial slots separated by a distance z_1 on a cylinder compare with the admittance and isolation between the same slots (separated by the same distance z_1) on a ground plane. A comparison is shown in Table II. We note that the self-admittance Y_{11} for the slot on the cylinder does not differ very vastly from that for the same slot in a ground plane, even though the cylinder circumference is only 1.5 wavelengths. Even the difference between the values of isolation is not very large.

Finally, let us consider the radiation pattern. Figures 4a and 4b show some typical θ cuts (for $\phi = o°$) for both a single slot and a pair of H-plane slots which are excited out of phase, but with equal amplitudes. Figure 4a shows the case when the cylinder is covered by a layer of lossy plasma and a dielectric. Figure 4b shows the case when the cylinder is covered by a very slightly lossy dielectric layer separated by a thin air gap from the cylinder surface. Note that in this case the pattern is peaked near $\theta = 0$, indicating the effect of surface wave modes.

Table II.

Comparison of Results for Slots on a Ground Plane with those on a Cylinder for $a = 3.6$, $b = 8.5$, $k = .418$, $\phi_o = 10°$, $\phi_1 = 0°$

FREE SPACE $Z_1 = 20$

Cylinder (2817)

Y_{11} (mho)	H-plane Isolation (db)
$1.56 \times 10^{-4} + j\,2.11 \times 10^{-4}$	46.0

Ground Plane 2656

Y_{11} (mho)	H-plane Isolation (db)
$1.93 \times 10^{-4} + j\,2.08 \times 10^{-4}$	44.0

PLASMA $_1 = 1 - j20$, $\Delta_1 = .0534$

Cylinder (2817)

Z_1	Y_{11} (mho)	Isolation (db)
15	$1.27 \times 10^{-3} + j\,2.44 \times 10^{-4}$	50.3
20	"	55.2
25	"	57.5

Ground Plane 2656

Y_{11} (mho)	Isolation (db)
$1.32 \times 10^{-3} + j\,2.52 \times 10^{-4}$	48.7
"	53.6
"	57.9

FIGURE 4a RADIATION PATTERN OF AXIAL SLOTS

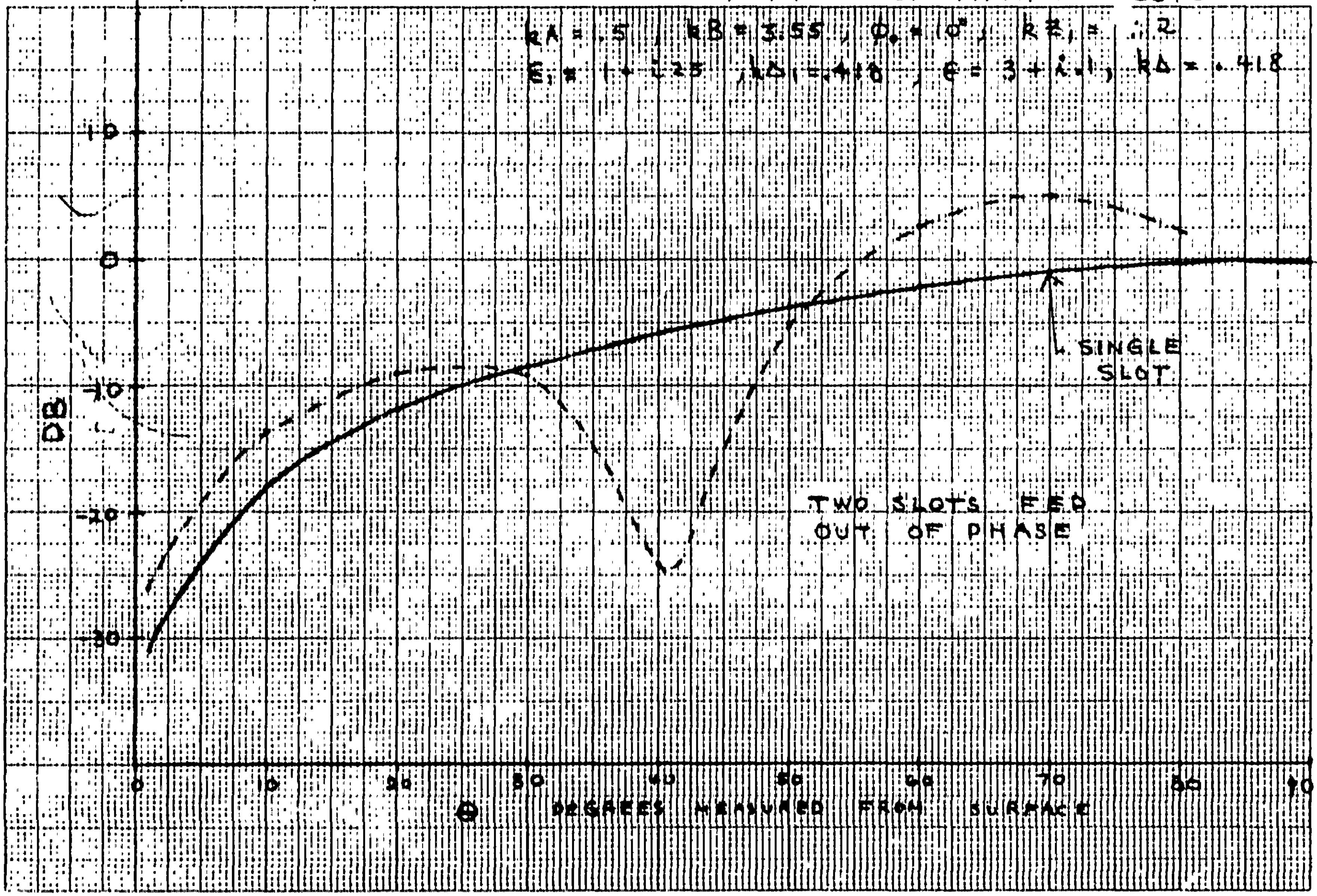

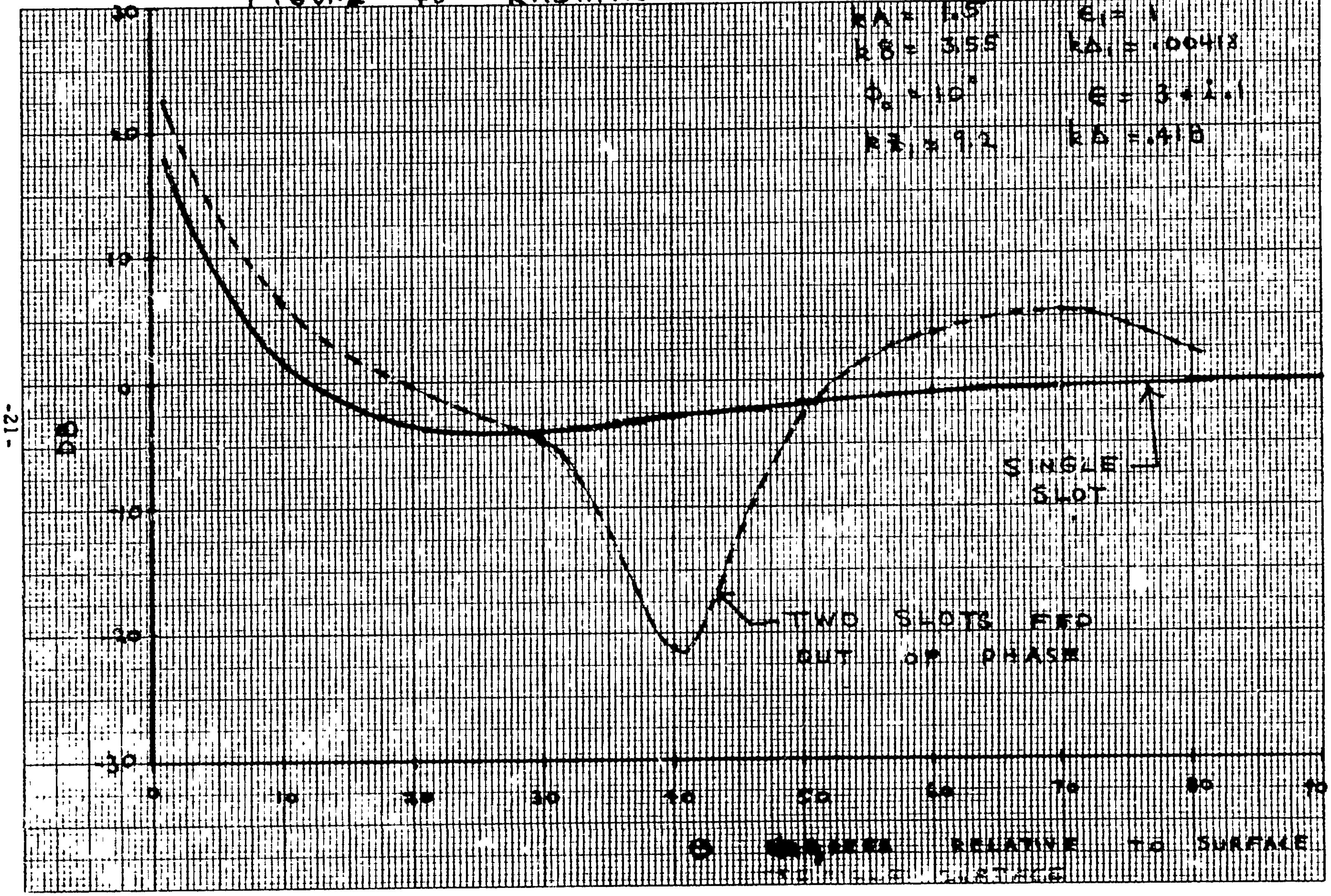

FIGURE 4b RADIATION PATTERN OF AXIAL SLOTS

2.2.2 Verification and Results from Options 3 and 4

To verify the validity of options 3 and 4 we have first considered the limiting case of a bare cylinder (for geometry see Figure 1b). For this problem some values have been computed by Swift et al (1969) of NASA. Table III is a comparison of their results with those from option 3 of program 2817. We note that the agreement is excellent. Also for $ka << 1$ we can compare 2817 with the theoretical admittance formula of Fante (1966) and Miller (1967) given by

$$Y_{11} = \frac{Y_o}{\ln\left(\frac{\Gamma ka}{\sqrt{2}}\right)} - i\left[\frac{-(.9)Y_o}{\ln\left(\frac{\Gamma ka}{\sqrt{2}}\right)} - 2\,ka\,Y_o \ln(kb)\right] \tag{12}$$

where Y_o is the admittance of free space and $\Gamma = 1.781$. The results of 2817 have been compared with (12), and the agreement was excellent.

To verify the validity of option 3 when the cylinder is covered by a plasma, we have again chosen a plasma which meets the conditions necessary for the thin sheath approximation to be valid. We take $a = 3$, $k = 1$, $b = .105$, $\Delta_1 = .02$ and $\epsilon_1 = 1 + i25$. The input admittance as predicted using the thin sheath approximation is

$$Y_{11} = 1.49 \times 10^{-3} - i\,3.44 \times 10^{-4} \quad \text{mho}$$

while the value obtained from program 2817 is

$$Y_{11} = 1.35 \times 10^{-3} - i\,4.0 \times 10^{-4} \quad \text{mho}$$

Again the agreement is favorable, and the differences are within those expected due to errors in using the sheath approximation.

Table III.

Comparison of admittances for an axial slot on a bare cylinder

ka	kb	Y_{11} (mho) Limit of .2817	Y_{11} (mho) NASA
1	.035	$.685 \times 10^{-4} + j\,1.49 \times 10^{-4}$	$.685 \times 10^{-4} + j\,1.49 \times 10^{-4}$
2	.070	$1.16 \times 10^{-4} + j\,2.52 \times 10^{-4}$	$1.16 \times 10^{-4} + j\,2.54 \times 10^{-4}$
3	.105	$1.62 \times 10^{-4} + j\,3.43 \times 10^{-4}$	$1.62 \times 10^{-4} + j\,3.44 \times 10^{-4}$

To verify the radiation patterns as predicted by option 4, we again first consider the free space limit. In this case (11) reduces to:

$$R = \frac{1}{\sin^2\theta\,\left[\mathrm{Ho}\,(ka\sin\theta)\right]^2}\left(\frac{\sin\left(\frac{kb}{2}\cos\theta\right)}{\frac{kb}{2}\cos\theta}\right)^2 \tag{13}$$

A comparison with the results of (13) with the results computed by option 4 of 2817 is given in Table IV.

To verify the validity of the computed radiation pattern when a plasma is present, we consider a plasma for which the thin sheath approximation is applicable. In that limit it can be theoretically shown (Fante, 1967) that if the aperture excitation is unchanged the pattern is also unchanged (both in amplitude and shape, except near $\theta = o$) from the vacuum situation when a plasma layer is present. Table V shows the ratio, R_p, of the radiation pattern with a plasma (satisfying the thin sheath criterion) to that in vacuum. We note that the ratio is generally near unity as is expected from the above theoretical considerations.

TABLE IV

Comparison of Theoretical and Computed Vacuum Radiation Patterns for $k = .25$, $a = 4$, $b = .140$. Values are Normalized to Unity at $\theta = 90°$.

θ (degrees)	R from 2817	R from equation (13)
20	3.48	3.49
30	2.20	2.21
40	1.64	1.64
50	1.34	1.34
60	1.17	1.17
70	1.07	1.07
80	1.05	1.05
90	1.0	1.0

TABLE V

Ratio R_P of the Radiation Pattern with a Plasma Layer (with $\epsilon_1 = 1 + i\,25$, $\Delta_1 = 0.1$) to the Vacuum Pattern for $a = 4$, $b = .140$, $k = .25$

R_P	θ (degrees)
.999	90
.998	80
.996	70
.991	60
.982	50
.967	40
.936	30
.860	20

2.3 Techniques for Computing the Bessel and Neumann Functions

Our method for computing Bessel functions is based on a technique described in the S.I.A.M. Review, Vol. 9 No. 1 January 1967, by Walter Gauschi. The article, entitled "Computational aspects of three-term recurrence relations" contains a complete description of the method and gives a full error analysis. The program will produce highly accurate Bessel functions provided the imaginary part of the argument is less than 174.673 in magnitude, and therefore no asymptotic expansions are necessary. Limiting forms are used for arguments whose magnitude is less than $1. \times 10^{-8}$, although this is not essential but merely faster.

The Neumann functions are computed using recursion upward (a numerically stable procedure) with starting values for $Y_0(z)$ and $Y_1(z)$ obtained by Neumann's expansion for Y_n in terms of J_i, $i = 1, 2, \ldots$.

Hankel functions $H_i^{(1)}(z)$ are computed as $J_i(z) + i\, Y_i(z)$ unless a loss of significance of six or more places will result. This occurs only for large, pure imaginary arguments. Here asymptotic expansions for $H^{(1)}(z)$ and $H^{(1)\prime}(z)$ are used. A reference for the Y and H expansions is the Handbook of Mathematical Functions published by the National Bureau of Standards, U.S. Dept. of Commerce.

3.0 Discussion of the Collision Frequency Approximation

In programs 2656 and 2817 we have neglected the effect of electric field strength on the electron-neutral collision frequency. It is readily shown that for the range of altitudes over which the signal attenuation is significant, this approximation is appropriate. Figure 5 shows the effective collision frequency, calculated from the Boltzmann equation model, as a function of E_e/p. For the 2 watt RANT S-Band slot, in the altitude regime between 130 kft and 40 kft, the slot conductance varies between 10^{-3} and 2×10^{-2} mhos/meter. As a result the electric field outside the antenna is, at most, of order

$$E = \left(\frac{2P}{abG}\right)^{1/2} \simeq \left[\frac{(2)\,(2)}{(2.54)(4.45) \times 10^{-3}}\right]^{1/2} \sim 18.7 \text{ v/cm}$$

At 130 kft the pressure, assuming $T = 4000°K$. is of order 30 torr. For lower altitudes the pressure will be higher. Thus, in the regime from to to 130 kft, where attenuation is most significant (and an accurate determination of ν_c important) the maximum value of E_e/p is of order

$$\frac{E_e}{p} \sim 1/2$$

Referring to Figure A. 1 we see that, since $E_e/p < 1/2$ for the 2 watt communications link, there is almost no error in approximating $\nu_c(E)$ by $\nu_c(E = 0)$.

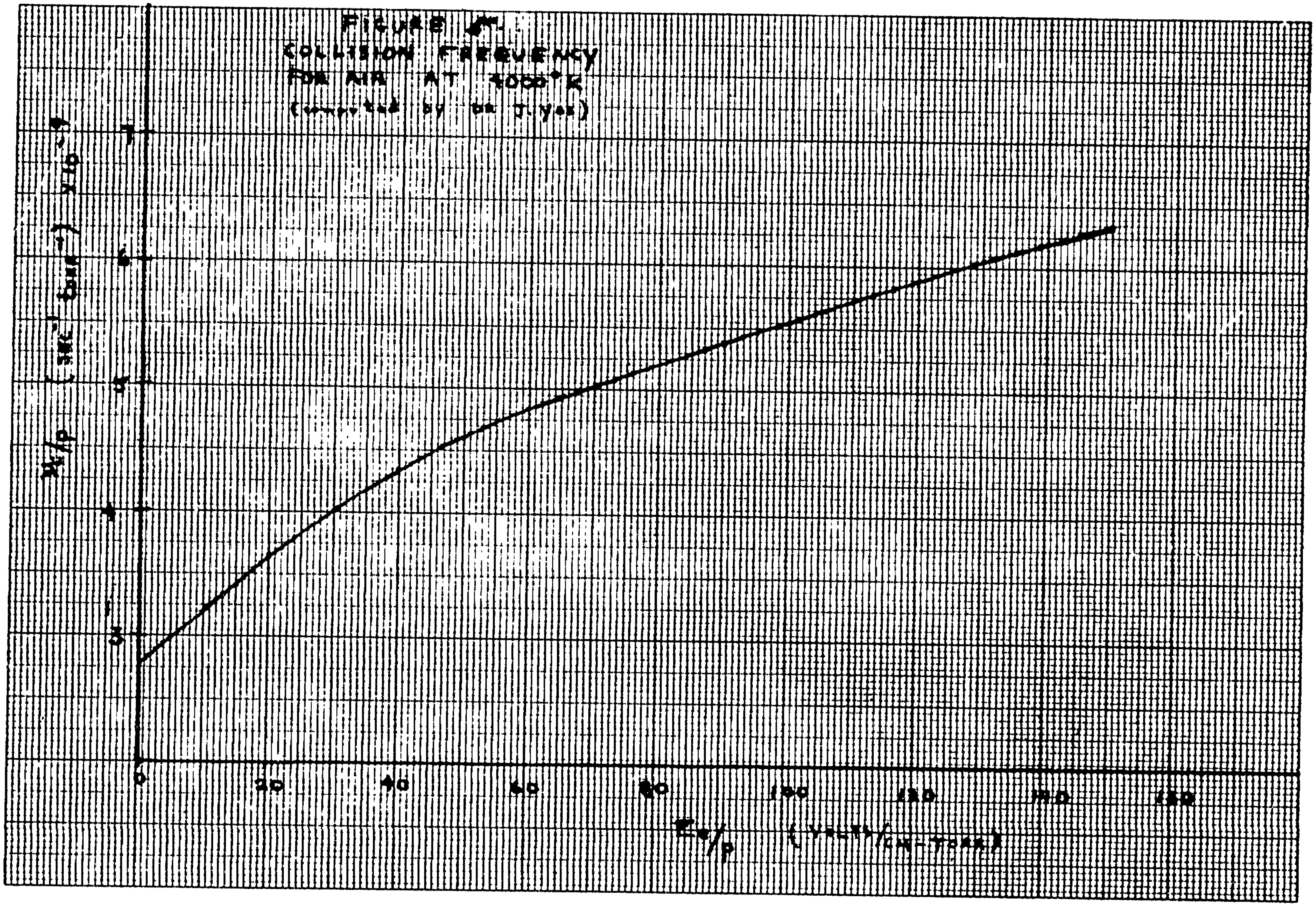

FIGURE
COLLISION FREQUENCY
FOR AIR AT 4000°K
(computed by Dr. J. Yos)

REFERENCES

Fante, R. L. [1966], Radio Science, Vol. 1, p1041-44 (also erratum, Radio Science, Vol. 1, p 1234).

Fante, R. L. [1967], Radio Science, Vol. 2, pp87-100.

Golden, K. and G. Stewart [1969], private communication

Knop C. etal [1965], presented at the Third Symposium on the Plasma Sheath, Boston, Massachusetts.

Miller, E. K. [1967], Radio Science, Vol. 2, pp1431-35.

Swift, C. T. etal [1969], IEEE Trans. AP-17, pp467-477.

APPENDIX A

DESCRIPTION OF GROUND PLANE LINEAR PLASMA COMPUTER PROGRAM

APPENDIX A

TABLE OF CONTENTS

PROGRAM 2656

*Described in Text of Report
**Submitted Separately

Program 2656 - Linear Ground Plane Plasma Model

Program 2656 calculates the admittance, isolation and radiation pattern for rectangular slots in a ground plane covered by an outwardly inhomogenous plasma.

PROGRAM 2656 - CORRELATION OF PROGRAM SEGMENT

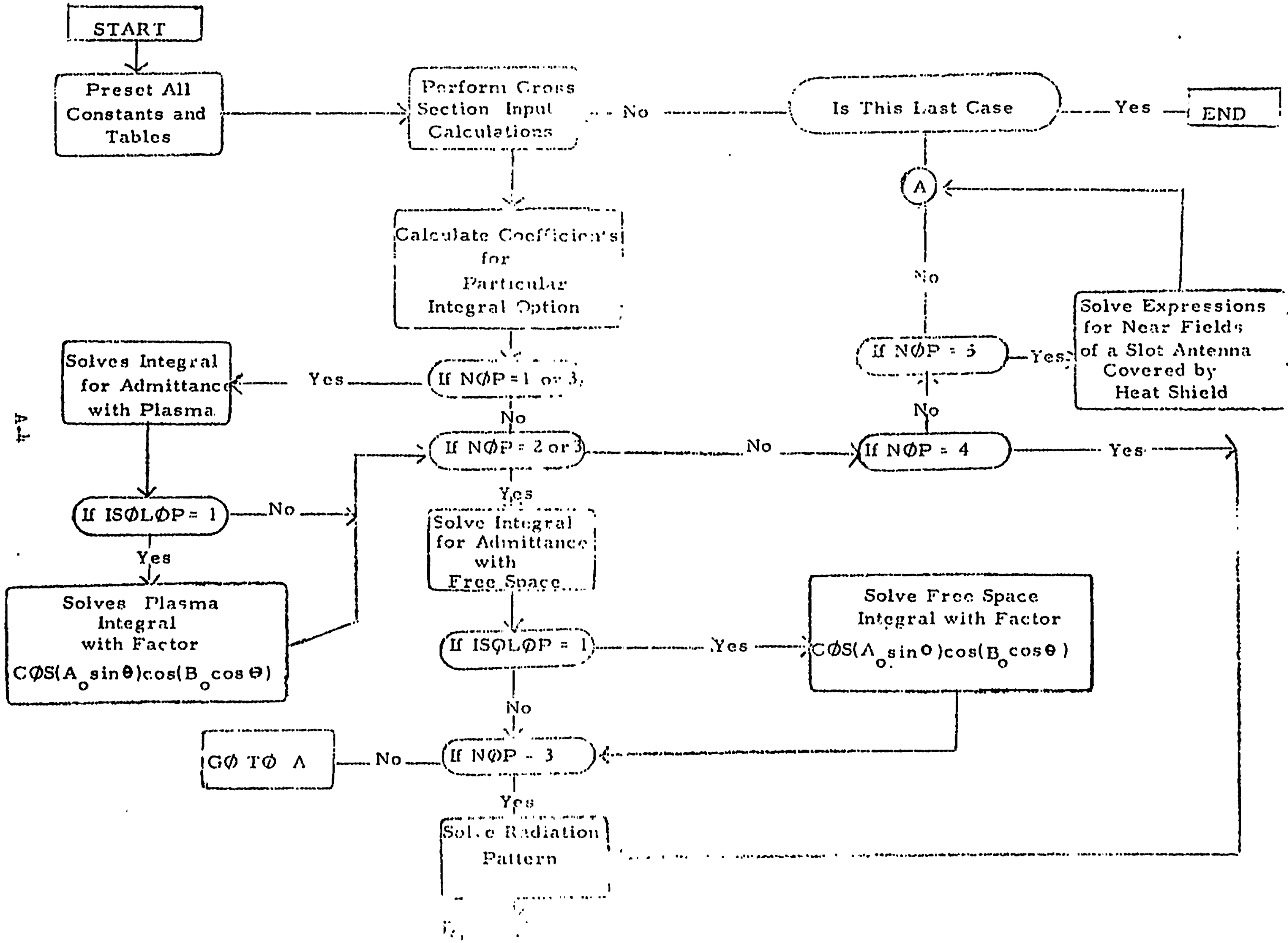

Program 2656

EXPLANATION OF INPUT

NUMD	Number of dielectric slabs. Maximum value is 100. Must be ≥ 1 if NOP is 1 or 3 or 4.
NLØNG	Optional input. NUMD may be trucated to conserve computer time in admittance calculation. NLØNG is then the total number of dielectric slabs.
NØP	Option: if = 1, then integral for admittance with plasma (Y'_o). if = 2, then integral for admittance with free space (Y'_{ov}). if = 3, both option 1 and 2 with complete printout of radiation pattern. if = 4, radiation pattern with admittance calculation; can include admittance by inputting XKP and/or XKV. if = 5, expressions for near fields of a slot antenna covered by a heat shield. Need x, y and z. If E_x, E_y, or E_z = 0 then XØP, YØP or ZØP must be 0 respectively.
ER	Used in formula as follows: $$Y_C = \left[ER - \left(\frac{\pi}{a\,k_o} \right)^2 \right]^{1/2} / 377$$ ER is relative dielectric constant of material inside wave guide. Preset to 1.
A	Large wave guide dimension in Cm.
B	Small wave guide dimension in Cm.
XAMBDA	Signal wave length in centimeters.
RAD	Factor defined D = D$\cdot$RAD
D	Thickness of each dielectric layer in Cm. Maximum of 100 values.

EPSR	Relative heat shield and plasma dielectric constant (real part). Maximum of 100 values. Not used in NØP2.
EPSI	Imaginary part of dielectric constant. Vector as above. Not used in NØP2.
NØR	Number of R's. $1 \leq$ NØR ≤ 100; used in NØP 3 or 4.
NTHETA*	Number of thetas. $1 \leq$ NTHETA ≤ 360; used in NØP 3 or 4.
NPHI	Number of phis. $1 \leq$ NPHI ≤ 360; used in NØP 3 or 4
R	Vector. Distance from antenna slot in meters. Maximum of 100 values. Used for NØP = 3 or 4 (preset to 1.)
THETA	Vector. Polar angle in degrees. (zero not permitted) Maximum of 360 values; used for NØP 3 or 4. $0 <$ THETA < 180; theta $\neq 90^{o}$.
PHI	Vector. Azimuth angle in degrees. (zero not permitted) Maximum of 360 values; used for NØP 3 or 4. $0 <$ PHI < 360; No multiples of 90^{o}.
XKP	Multiplying factor. $\lvert 1 + R_P \rvert^2$ times XKP replaces $\lvert 1 + R_P \rvert^2$ in NØP 3 or 4. However, in NØP4 $R_P = 0$. (XKP preset to 1.)
XKV	Multiplying factor $\lvert 1 + R_V \rvert^2$ times XKV replaces $\lvert 1 + R_V \rvert^2$ in NØP 3 or 4. However, in NØP 4 $R_V = 0$. (XKV preset to 1.)
IREND	Number of successively larger R's to be used in integrals (Preset to 20).
RINFCN	Convergence criterion for integrals as $R \rightarrow \infty$, preset to .01
NPLT2P	Plot option for (N_r) 2p. If = 1 plots; if = 0 no plots. (preset to 0)
NPLTNV	Plot option for $(N_r)_V$. If = 1 plots; if = 0 no plots. (Preset to 0)
NPLTN2	Plot option for $(N_r)_{2p} / (N_r)_V$. If = 1 plots; if = 0 no plots. (Preset to 0)

LØGR	Option: if = 1 then polar plot of R is linear. if = 2 then $\log_e R$. (preset to 1).
NV2*	Option: if = 1 then points of plots are not connected. if = 2 then connected (preset to 2).
TITNRP	56 character title for $(N_r)_{2p}$ polar plot. The title must appear on the second card. Requires 2 cards if used.
TITNV	56 character title for $(N_r)_V$ polar plot. Requires 2 cards if used.
TITN2	56 character title for $(N_r)_{2p}/(N_r)_V$ polar plot. Requires 2 cards if used.
EPSIH	Optional input. Imaginary part of heat shield dielectric constant. Can be used only if INØP $\neq$ 3.
EPSRH	Optional input. Real part of heat shield dielectric constant.
PG	Boundary layer pressure, atmospheres.
RATEMP	Factor multiplying temperature points. Preset to 1.
RADEN	Factor multiplying density ratios. Preset to 1.
EL	Ionization potential, ℓ^{th} electrophillic negative ion.
GL	Ratio of electronic weighting factors of each electrophillic species.
PL	Partial pressure of ℓ^{th} electrophillic species.
NL	Number of electrophillic species. Maximum of 10.
TEMP	Temperature of each plasma layer, deg K, maximum of 99 values.
DENSRA	Density ratio of each plasma layer.
EMC	Ratio of heat shield density to total gas density in each plasma layer.
ELEDEN	Electric density of each plasma layer, particle/cm^3.
CØLFRE	Collision frequency of each plasma layer, rad/sec.
EI	Ionization potential of i^{th} contaminant, ev.

EMI	Parts Per Million of i^{th} contaminant.
GI	$\frac{g + ge}{gi}$, ratio of electronic weighting factors of each contaminant.
WI	Atomic weight of each contaminant
NI	Number of contaminants. Maximum of 10.
INØP	3 input EPSR and EPSI 2 input ELEDEN and CØLFRE 1 input ELEDEN, TEMP and DENSRA 0 input TEMP and DENSRA (program computes clear air values of ELEDEN and CØLFRE) -1 input TEMP, DENSRA, EMC, EMI, EI, GI, WI, NI (program computes ELEDEN only due to contaminants and COLFRE for air) -2 input same as -1 (program includes effect of air on ELEDEN)
ISØLØP	Option: If set to 1 then the factor $\cos(A_o \sin\theta) \cos(B_o \cos\theta)$ is also used in the integrand for NØP = 1 and/or NØP = 2
A0	The H plane slot separation in cm. Needed for ISØLØP = 1 and GAMMA calculation in NØP 3 and 4. Preset to 0.
B0	The E plane slot separation in cm. Needed for ISØLØP = 1 and GAMMA calculation in NØP 3 and 4. Preset to 0.
EPSIL	When ZØP = 1. and EPSR = 1. and EPSI = 0. , the relative interval (ϵ) in ρ used at singularity. Also used for NØP 2. Preset to .1
NØXYZ	The number of x, y and z's to be inputted.
X Y Z	Vectors. In $E_x(x, y, z)$, $E_y(x, y, z)$ and $E_z(x, y, z)$. Used only in NØP = 5 Maximum of 100 values
XØP	Option. If = 0. then convergence not used in solution of E_x. If = 1. then convergence used. Preset to 1. If $E_x = 0$ XØP must be 0.

YØP ZØP	Option. Same as XØP but explanations apply to E_y and E_z respectively.
NØDBLE	The maximum number of doubling of points in the Simpsons' integral solution. Preset to 8. If greater accuracy required, use 10 or 12 but problem will increase in time radically.
THTCNV	Theta convergence criterion. Preset to .005
ISKIP	Option: If = 1 and if ISØLØP = 1 this causes the suppression of the Y_o calculation. Y_o value used in the ISØL calculation can either be inputted or the last value from a previous case will be used. (Preset to 0)
YREAL1	The real part of Y_o for NØP = 1. Used when ISKIP = 1
YIMAG1	The imaginary part of Y_o for NØP = 1. Used when ISKIP = 1
YREAL2	The real part of Y_o for NØP = 2. Used when ISKIP = 1
YIMAG2	The imaginary part of Y_o for NØP = 2. Used when ISKIP = 1

Note: Calculated values of ELEDEN and CØLFRE assume equilibrium, EPSHR and EPSIH may be used only when INØP $\neq$ 3.

OUTPUT

The input program outputs the card images of the input.

OUTPUT NAME	DEFINITION
Y0'	Real and Imaginary part of Self Admittance
Y12	Real and Imaginary part of Mutual Admittance
ISØL	Isolation in DB
YG	Wave Guide Characteristic Admittance
Y0V'	Vacuum Self Admittance
(NR)P	Radiation Pattern with Plasma
(NR)V	Vacuum Radiation Pattern

OPERATION INSTRUCTIONS FOR PROGRAM 2656

Program 2656 computes the self* and mutual admittances of unmatched rectangular slots on a plasma covered ground plane. Attached here is an input sheet and a complete explanation of all inputs. We have also included three sample outputs. Exhibit A is a case where the admittance and isolation are computed for a two layer lossy dielectric (or plasma). Exhibit B computes the admittance and isolation for a ground plane covered by a slightly lossy dielectric. We note that in this case the program prints out a statement that the integral did not converge in a given region due to the tight convergence criteria we have imposed. If the real parts are within about 5% of each other and the imaginary parts are also within about 5% of each other, the error in Y_{11} and Y_{12} is usually less than 1%. If the real or imaginary parts differ by more than 5%, the user should increase NØDBLE. Exhibit C illustrates the case when the admittance, radiation pattern and attenuation are calculated for a multilayer plasma.

Also included in this package is the complete deck. This deck is appropriate for use on the IBM 360-75.

*Note that e^{-jwt} dependence is assumed. Thus 2656 values for admittance are complex conjugate of those for e^{+jwt}.

APPENDIX B

DESCRIPTION OF CYLINDER LINEAR PLASMA COMPUTER PROGRAM

APPENDIX B

TABLE OF CONTENTS

PROGRAM 2817

*Described in Text of Report
**Submitted Separately

PURPOSE OF PROGRAM 2817

Cylinder Linear Plasma Model

Program 2817 computes the admittance isolation and radiation pattern for slots on an infinite plasma covered cylinder. The program has four options: Option 1 calculates the admittance and isolation for a pair of axial slots, option 2 calculates the radiation pattern for the above case, option 3 calculates the admittance of a circumferential gap, and option 4 calculates the radiation pattern for the circumferential gap.

Program 2817 - Correlation of Program Segments

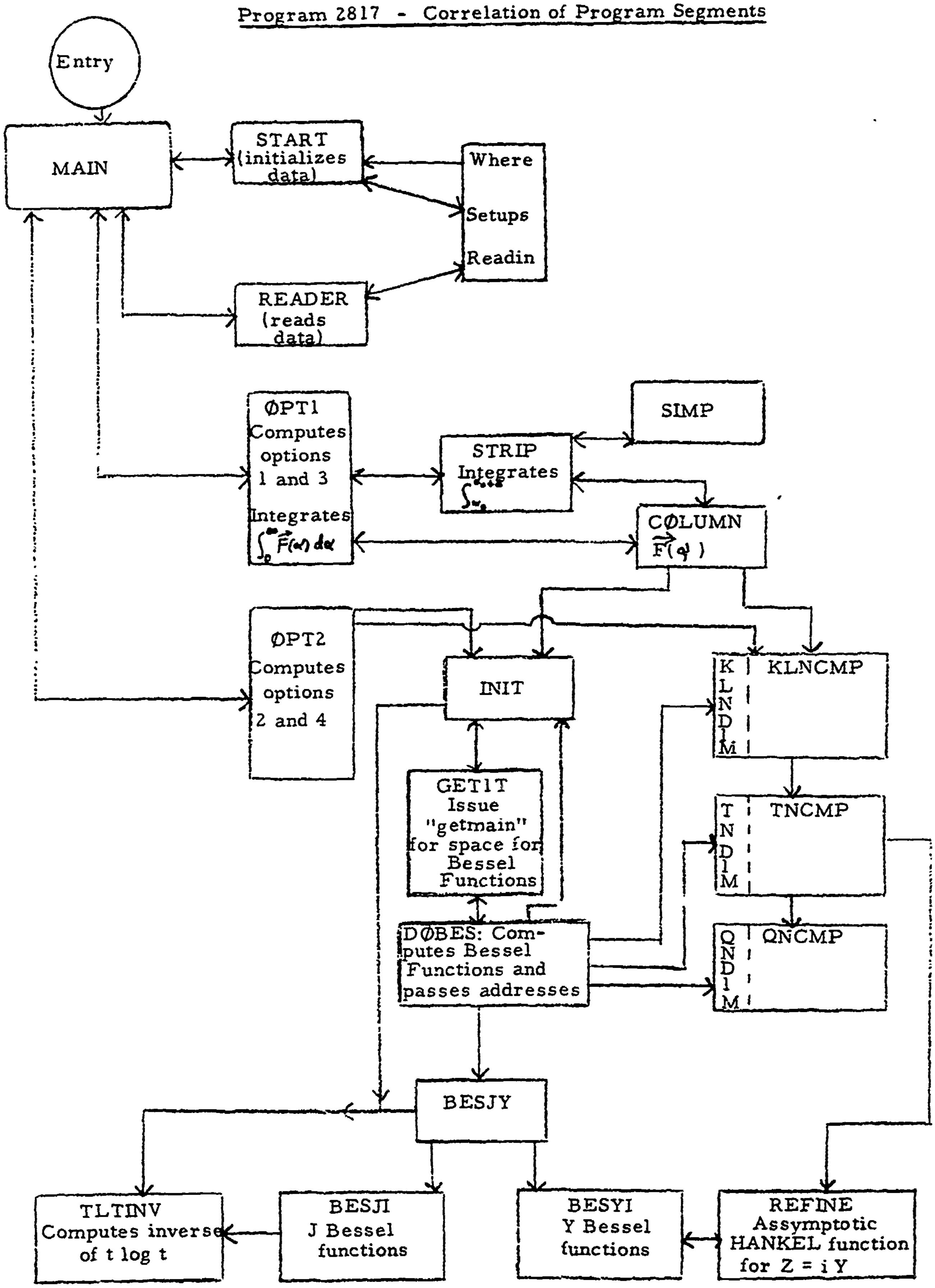

DIGITAL COMPUTER INPUT REQUEST FORM	PROBLEM NO. 2817	MEMO NO.	SECTION NO.	CONTINUATION SHEET

EXPLANATION OF INPUTS

A	Radius of the bare cylinder.
B	Slot width in the axial direction.
BETA	Amplitude of the excitation of slot 2 relative to that of slot 1.
CØMPARE	When running option 4, shall the pattern be compared to one for $\epsilon = (1, 0)$. Answer .YES or .NØ .
DELTA1	Thickness of the heat shield.
DELTA	Incremental thickness of the plasma layers.
EPSILØN	Relative dielectric constant. (List the real and imaginary part for each layer covering the bare cylinder.)
K	Free space wavenumber.
LAMBDA	Phase of slot 2 relative to slot 1.
PHI0	Angular width of the aperture in degrees.
PHI1	Azimuthal separation of the centers of slots 1 and 2, in degrees.
Z1	Axial separation of the centers of slots 1 and 2, in degrees.
NLAYERS	Total number of layers (heat shield plus plasma).
PHI	Value or values of ϕ for radiation pattern.
THETA	Value or values of θ for radiation pattern. Values may be listed or given in STARTING(INCREMENT)FINAL format. EXAMPLE: 1.(1.)10.(2.)80.(1.)89.
ØPTIØN	Use 1 if we desire a calculation of Y11, Y12 and isolation for axial slot.
	Use 2 if we desire radiation pattern only for a single slot and a pair or axial slots.
	Use 3 if we desire a calculation of Y11, Y12 and isolation for a circumferential slot.
	Use 4 if we desire the radiation pattern of a circumferential slot.

HAD 2-0963 5-63

DIGITAL COMPUTER INPUT REQUEST FORM	PROBLEM NO: 2817	PROGRAMMER: R. Elkin
	TITLE:	

MEMO NO.	SECTION NO.	WORK ORDER NO.	(E240 USE ONLY)	REQUESTED BY:	EXT.	EST. TIME	PAGE 1 OF 2 PAGES

NAME / ____________ DATE/ ____________ BIN / ____________

SECTIØN / ____________ MEMØ / ____________ CASE / ____________

ØPTIØN ____________ NLAYERS ____________

EPSILØN ____

____

A ____________ B ____________ K ____________

DELTA ____________ DELTA1 ____________ PHI0 ____________

PHI1 ____________ Z1 ____________ BETA ____________

LAMBDA ____________

PHI ____

____

THETA ____

____

CØMPARE ____________

EXPLANATION OF OUTPUT SYMBOLS

Y_{11}	The self admittance
Y_{12}	The mutual admittance
Y_G	The waveguide characteristic admittance
ISOL	The isolation in db
R_1	The far radial Poynting vector of a single slot
R_2	The far radial Poynting vector for a pair of slots

APPENDIX C

DESCRIPTION OF PROBE-FED CAVITY COMPUTER PROGRAM

APPENDIX C

TABLE OF CONTENTS

Program OK-5

*Described in Text of Report
**Submitted Separately

PURPOSE OF PROGRAM OK-5

Program OK-5 was written to modify the attenuation and isolation calculated by Avco computer program 2656 to account for:

1. The fact that the S- and C-band experiment antennas are not infinite waveguides but cavity backed slots.

2. The fact that there may be a lossless tuning network in the transmission line feeding the probe.

Multiple cases can be run by stacking one case behind the other. No "// XEQ" card is necessary between cases. After the last data card of the last case being run a card with a "1" punched in column two should be used in order to properly terminate program execution.

Flow Chart for Program OK-5

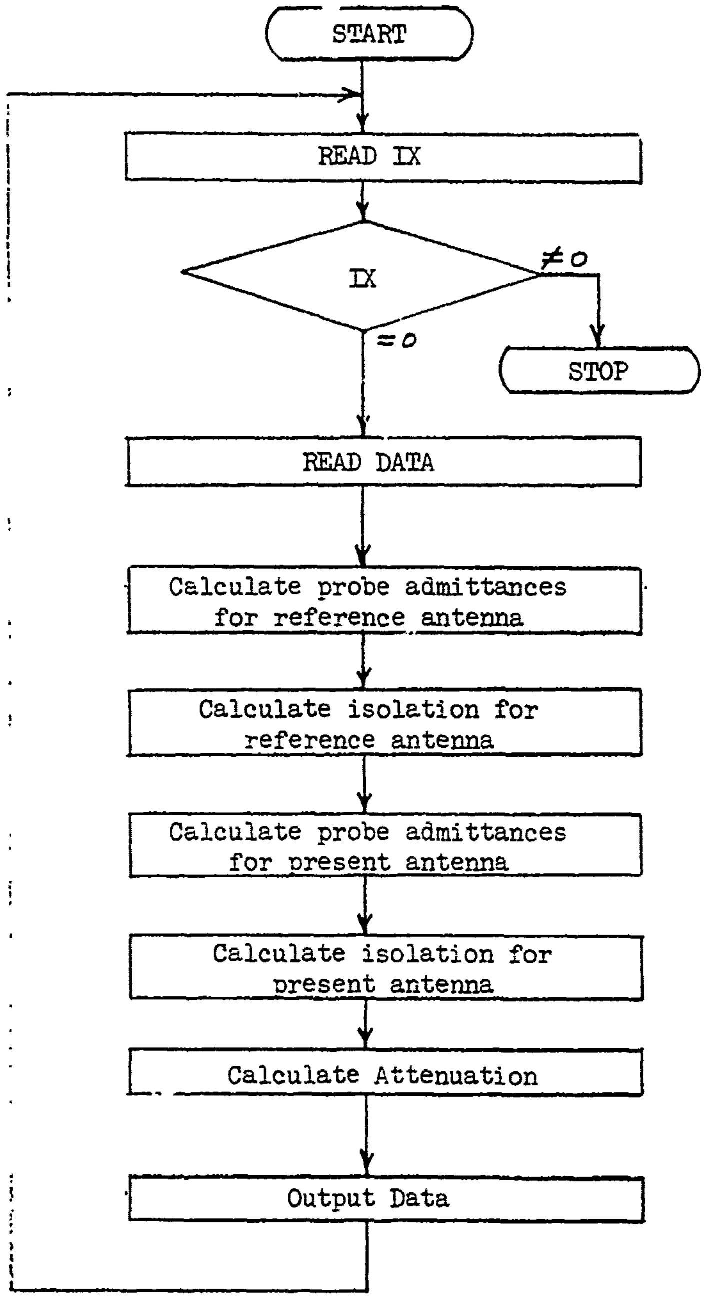

Input Format Description For OK-5

Input Description	Symbol	Card	Columns	Format	Typical Value
Code Word When set to "1" program stops	IX	1	1 - 2	I2	0
Title of Case	IT	1	3 - 43	20A2	TEFLON, etc.
Attenuation outputed from 2656 when reference antenna is radiating into the reference environment	A2656	2	1 - 10	F10.0	-0.7369
|1+RP| **2 Transmission Coefficient for A2656 Attenuation	OPRPA	2	11 - 20	F10.0	2.28611
Attenuation Outputed From 2656 When Subject Antenna is Radiating Into Present Environment	B2656	3	1 - 10	F10.0	-0.7043
|1+RP| **2 Transmission Coefficient for B2656 Attenuation	OPRPB	3	11 - 20	F10.0	2.27707
Complex Aperture Self-Admittance to Which Reference Antenna is Matched	Y11OR	4	1 - 20	2F10.0	0.001071 0.0005976
Complex Aperture Mutual-Admittance to Which Reference Antenna is Matched	Y12OR	4	21 - 40	2F10.0	0.0 0.0
Complex Aperture Self-Admittance into Which Reference Antenna is Radiating	Y11R	5	1 - 20	2F10.0	0.001071 0.0005976
Complex Aperture Mutual-Admittance into Which Reference Antenna is Radiating	Y12R	5	21 - 40	2F10.0	0.00004792 -0.0001681

Input Description	Symbol	Card	Columns	Format	Typical Value
Complex Aperture Self-Admittance to Which Subject Antenna is Matched	Y110	6	1 - 20	2F10.0	0.001071 0.0005976
Complex Aperture Mutual-Admittance to Which Subject Antenna is Matched	Y120	6	21 - 40	2F10.0	0.0 0.0
Complex Aperture Self-Admittance into which subject antenna is Radiating	Y11	7	1 - 20	2F10.0	0.001081 0.0005911
Complex Aperture Mutual-Admittance into which Subject Antenna is Radiating	Y12	7	21 - 40	2F10.0	0.00004745 -0.0001674
Aperture Length (cm)	A	8	1 - 10	F10.0	4.44
Aperture Width (cm)	B	8	11 - 20	F10.0	2.54
Length of Probe in Cavity (cm)	D	8	21 - 30	F10.0	2.0
Probe Radius (cm)	R	8	31 - 40	F10.0	0.159
Distance From Probe to Back of Cavity (cm)	ALL	8	41 - 50	F10.0	2.0
Distance From Probe to Aperture (cm)	ABL	8	51 - 60	F10.0	2.44
Relative Dielectric Coefficient for Cavity	EPS	9	1 - 10	F10.0	3.75
Characteristic Admittance of Line Feeding the Probe	YP	9	11 - 20	F10.0	0.02
Free Space Wavelength of Signal (cm)	ALMDA	9	21 - 30	F10.0	12.766

OK-5 Output Description

Item	Description
1-4	Input
5	Magnitude of the reflection coefficient squared for the reference antenna.
6	Magnitude of the transmission coefficient squared for the reference antenna.
7	Reflection loss in dB's for the reference antenna.
8	Isolation in dB's for the reference antenna.
9	Input
10	Magnitude of the reflection coefficient sqared for the subject antenna.
11	Magnitude of the transmission coefficient squared for the subject antenna.
12	Reflection loss in dB's for the subject antenna.
13	Isolation in dB's for the subject antenna.
14	Attenuation loss in dB's. Given by $\text{Attenuation} = -10\text{LOG}_{10}\left(\frac{\text{Power radiated by subject antenna}}{\text{Power radiated by reference antenna}}\right)$

OK-5 INPUT DATA CARDS FOR A TYPICAL CASE

```
   TEFLON   S-BAND   150KFT   NEAR-H
  -0.7369   2.28611                                                S   R
  -0.7043   2.2[illegible]707                                           150 S   P
  0.001071  0.0005976 0.0         0.0                              S-BAND
  0.001071  0.0005976 0.00004792-.0001681                          S NEAR-H
  0.001071  0.0005976 0.0         0.0                              S-BAND
 0.001081   0.0005911 0.00004745-0.0001674                         150 S NH
 4.44       2.54      2.0         0.159      2.0        2.44
 3.75       0.[illegible]2      12.766
 -1
```

OK-5 OUTPUT

1 TEFLON S-BAND 150KFT NEAR-H

2 SLOT PARAMETERS

```
SLOT LENGTH      =   4.440     SLOT WIDTH      =   2.540
PROBE DEPTH      =   2.000     PROBE RADIUS    =   0.159
PROBE TO BACK    =   2.000     PROBE TO FRONT  =   2.440
PROBE ADMITT.    =   0.070     DI-ELECTRIC     =   3.750
WAVELENGTH       =  12.766
```

3 OUTPUT FROM 2656

```
REFERENCE ENVIRONMENT    ATTENUATION =  -0.7369
                         /1+RP/**2   =  2.28611

PRESENT ENVIRONMENT      ATTENUATION =  -0.7043
                         /1+RP/**2   =  2.27707
```

REFERENCE ANTENNA

```
4 APERTURE ADMITTANCE    MATCHED TO  =  0.0010710   + I (  0.0005976 )
                                        0.0000000   + I (  0.0000000 )
                         PRESENT     =  0.0010710   + I (  0.0005976 )
                                        0.0000479   + I ( -0.0001681 )

5 /R/**2            =  0.000119     6 /1+R/**2     =  1.007676
7 REFLECTION LOSS   =  0.0005       8 ISOLATION    =  21.8147
```

SUBJECT ANTENNA

```
9 APERTURE ADMITTANCE    MATCHED TO  =  0.0010710   + I (  0.0005976 )
                                        0.0000000   + I (  0.0000000 )
                         PRESENT     =  0.0010910   + I (  0.0005911 )
                                        0.0000474   + I ( -0.0001674 )

10 /R/**2           =  0.000246     11 /1+R/**2    =  1.005526
12 REFLECTION LOSS  =  0.0010       13 ISOLATION   =  21.9347
```

14 ATTENUATION (DB) = 0.0233